KSME Journal, Vol. 10, No. 2, pp. 235~245, 1996

On the Breakup Mechanisms of Air-Assisted Drops in a High Speed Air

Sang-Soon Hwang*

(*Received September 22, 1995*)

An experimental study was performed to investigate break-up mechanisms of liquid drops injected into a transverse high velocity air jet. The range of conditions included the three drop breakup regimes previously referred to as bag, shear or boundary layer stripping, and 'catastrophic' breakup regimes. The results show that the break-up mechanism consists of a series of processes in which dynamic pressure effects deform the drop into a thin liquid sheet. The flattened drop subsequently breaks up into small droplets. At high relative velocity, in the 'catastrophic' breakup regime, drops are flattened and fragmented by relatively large wavelength waves whose wavelengths and growth rates are consistent with estimates from Rayleigh-Taylor instability theory. The minute drops that are also produced at this high relative velocity appear to originate from short wave length of Kelvin-Helmholtz waves growing on the larger liquid fragments.

Key Words: Drop Breakup, Drop Generator, Instability Wave, Breakup Regimes, Weber Number

Nomenclature

B_1 : Breakup time constant
Re : Reynolds number, Ud/ν
T : Taylor parameter, $ZW_{e2}^{0.5}$
t : Time
U : Air-liquid relative velocity
V : Liquid injection velocity, volume
We : Weber number, $\rho U^2 d/\sigma$
Z : Ohnesorge number, $\mu_L/(\rho_L d\sigma)^{1/2}$
λ : Wavelength, RT wavelength
μ : Viscosity
ω : Wave growth rate, RT wave growth rate
$\bar{\omega}$: Frequency
ν : Kinematic viscosity
ρ : Fluid density
σ : Surface tension
Λ : KH wavelength of the most unstable surface waves
Ω : KH growth rate of the most unstable surface waves

Subscripts

1 : Liquid phase
2 : Gas phase
bu : Breakup
d : Drop
g : Gas
j : Jet
L : Liquid

* Dept. of Mechanical Engineering, University of Inchon, Korea

1. Introduction

Liquid atomization is widely used in a variety of applications such as gasoline and diesel engines. It is well known that the combustion efficiency and pollutant emissions from engines are influenced by the rate of vaporization of the liquid fuel, which is greatly dependent on the liquid atomization process. Atomization is enhanced by imposing a high relative velocity between liquid and ambient gas. The high relative velocity is achieved in diesel engines by utilizing the high fuel injection pressure. In air-assist or air-blast

injector systems supply of high pressure air is required to generate the high-relative-velocity air flow.

Many basic studies of the atomization process have been performed. Reviews of these studies have been provided by Krzeczkowski (1980), Reitz and Bracco (1986), Pilch et al. (1987), Hsiang and Faeth (1992). At lower velocities, the growth of small disturbances on the liquid surface due to the interaction between liquid and ambient gas is believed to be a dominant reason for the liquid breakup. The most unstable wavelength and breakup drop size are predicted well by linear theories (e. g., Rayleigh, 1878; Mahoney and Sterling, 1978). As the jet velocity is increased and aerodynamic effects become more important, there are more complexities in breakup mechanisms.

For drop breakup, most researches have been made in understanding the breakup of relatively low speed drops. As the relative velocity between drop and gas is increased, various drop breakup regimes are encountered, that have been referred to as bag breakup (Kennedy and Roberts, 1990), shear breakup (Ranger and Nicholls, 1969), and the so-called 'catastrophic' breakup (Reinecke and Waldman, 1970) regimes. As the relative velocity between drop and surrounding gas is increased, the drop distorts from its undisturbed spherical shape and becomes flattened, or disk shaped, normal to the flow direction. The velocity of the gas has a maximum near the equator and equals zero at the drop's poles (the stagnation point). Thus, the Bernoulli gas pressure is higher at the poles, which causes flattening of the drop. At sufficiently high velocity, the drop becomes thin enough that the center of the disk deforms into a thin balloon- or bag-like structure which is stretched and swept off in the downstream direction. The rupture of the bag produces small droplets, while the liquid locted in the rim of the distorted disk-shaped drop eventually breaks up into relatively large drops.

At high relative velocity, droplet breakup mechanism is less well understood. The breakup process produces small drops which appear to be sheared off from the parent liquid drop, hence the term of shear breakup regime. Liu and Reitz(1993) have shown that in the 'catastrophic' regime the drop also flattens and that the unstable growth of short wavelength surface waves is involved in the breakup process. These waves are stretched into ligaments by the high speed air flow. The high-velocity drop breakup mechanism was thought to be similar to the breakup mechanism of high velocity jets in the second wind-induced and possibly also the atomization regimes, which also involve the unstable growth of short wavelength surface waves and the formation of fibers or ligaments.

Criteria for drop breakup regime transitions in steady high-speed gas flows have been presented by Krzeczkowski (1980) and other authors. The Weber number and the Ohnesorge number $Z=\mu_L/(\rho_L d\sigma)^{1/2}$ (where μ_L is the liquid viscosity, and ρ_L is the liquid density) have been found to be important parameters. For example, for Ohnesorge numbers less than one ($Z<1$, i. e., all but the most viscous fluids) significant drop distortion and oscillation are noticed starting at $We_g \sim 1$ (the Weber number is based on the undisturbed drop diameter). Bag breakup commences at about $We_2=12$. Transition to shear type breakup occurs at higher Weber numbers ($We_g>80$) and 'multimode' breakup (combined bag- and shear-type) occurs in intermediate Weber number range. For high viscosity liquids the Ohnesorge number must be introduced and the breakup regime transitions are moved to higher Weber numbers(Wu et al., 1993).

In general, linear models based on the infinitesimal disturbance instability theory can be applied to predict the drop size of liquid jets at low velocities. But, as the air velocity increases, aerodynamic and possibly viscous effects become more important and the process is more difficult to analyze. Thus, there are many uncertainties about the break-up mechanisms for high velocity jets and drops.

The objective of the present work is to investigate break-up mechanisms of liquid drops injected into a high relative velocity air flow and verify the results of previous works for drop breakup mechanism in high relative velocity. The experi-

mental approach used double-pulsed high-magnification photography to reveal the temporal progress of the break-up of the drops. The conditions tested correspond to a drop Weber number range from 56 to 463 and thus cover all of bag, shear and catastrophic breakup regimes.

2. Experimental Details

The experimental apparatus consisted of a liquid drop generator and an air nozzle with a converging exit, which were arranged in a cross flow pattern as shown in Fig. 1. The injections were into ambient air. The air nozzle exit was a rectangular slit with $h=1.3$ mm and $b=10$ mm, where h is the slit width and b is the slit length (i. e., into the plane of the paper in Fig. 1). The 5 mm long nozzle passage featured a rounded entrance with radius $R=5$ mm (i. e., $R/b=0.5$) to ensure that the velocity profile at the nozzle exit was flat so that mixing and shear layer effects could be neglected. By injecting drops close to the nozzle exit plane (1.5 mm from the exit plane) the shear layer thickness at the edge of the jet is estimated to less than 1 drop diameter and the time needed for the drop to traverse the shear layer is much less than one oscillation period of the drop (Liu and Reitz, 1993).

The monodisperse droplet stream was generated using a Berglund-Liu vibrating orifice drop generator (Berglund and Liu, 1973). The drop size generated was determined from the relationship

$$d=\left(\frac{6Q}{\pi f}\right)^{1/3}$$

where Q is volumetric flow rate and f is the applied frequency. In this study the drop size was 189 μm and f was 40 kHz. The piezo-electric drop generator was operated using a square wave signal with a peak-to-peak voltage of 20 V. The liquid injection pressure was 275 kPa, and, under these conditions, a drop was ejected every 25 μs at a velocity of 16 m/s.

The fuel used was Benz oil UCF-1 test fuel which meets SAE J967d, ISO 4113 (a diesel-type fuel). The technical specifications of the fuel were: viscosity 0.00212 Ns/m^2, density 824 kg/m^3, surface tension 0.02 kg/s^2, flash point 348 K, and t-90 distillation point 483 K.

Figure 2 shows the optical system which consisted of two Xenon high intensity nano-pulse light sources and a Nikon 35 mm camera equipped with a Questar QM-100 ling distance microscope lens. In double-pulse operation two prisms were used to redirect the nano-lamp light sources as shown. The time interval between two pulses was controlled using an Avionics Model 111AR time delay generator. The pulse durations were different for the two nano-lamps (10 and 20 ns Xenon Models N787B and N789B, respectively). This difference in pulse duration produced different exposures on the film which was useful for time sequencing of the images. High sensitivity Kodak T-Max 400 film was used for the photography. The magnification was $\times 15$ on the film negatives. It was of interest to photograph the drops later in the breakup process as well. For this purpose a second field-of-view was used that

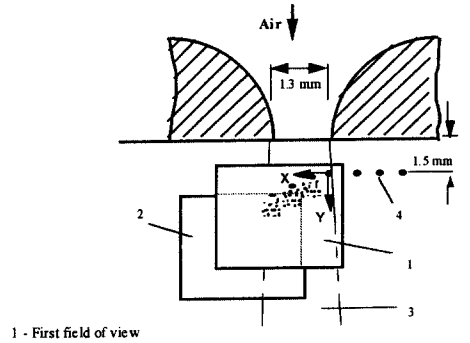

Fig. 1 Schematic diagram of experimental apparatus

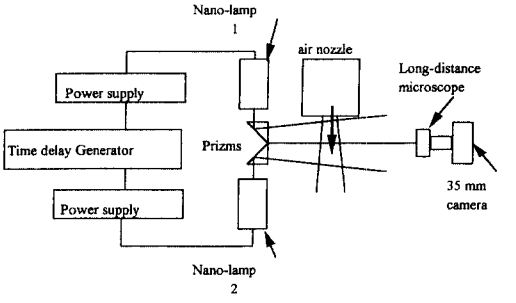

Fig. 2 Schematic diagram of optical layout for double-pulse photography

Table 1 Experimental conditions and variables

Case	Air velocity(m/s)	Air temperature(K)	Weber number	Reynolds number
1	77	293	56	900
2	150	293	260	1930
3	200	293	463	2573

was displaced about 0.5 mm in the X and Y directions, as indicated in Fig. 1.

The breakup regimes are classfied into three regimes which are called the bag, shear and 'catastrophic' rigimes (Liu and Reitz, 1993). Three air flow velocities representative of these regimes were selected as 70 m/s(bag), 150 m/s(shear), 200 m/s(catastrophic). The operating variables of each case are summarized in Table 1.

3. Breakup Model

3.1 TAB Breakup model

O'Rourke and Amsden (1987) proposed a drop breakup model called the "TAB" (Taylor Analogy Breakup) model which is based on Taylor's (1963) analogy between an oscillating and distorting drop and a spring-mass system. The external force acting on the mass, the restoring force of the spring, and the damping force are analogous to the gas aerodynamic force, the liquid surface tension force, and the liquid viscosity force, respectively.

In the TAB model the distortion parameter, $y=2x/r$(x is the displacement of the equator of the drop from its equilibrium position), is calculated by solving the spring-mass analogy equation,

$$\ddot{y}=\frac{2}{3}\frac{\rho_g U^2}{\rho_l r^2}-\frac{8\sigma}{\rho_l r^3}y-\frac{5\mu_l}{\rho_l r^2}\dot{y} \tag{1}$$

where μ_l is the liquid viscosity and the dot indicates a time derivative. If it is assumed that the relative velocity of the drop and the gas, U is constant, then the solution to Eq. (1) is

$$y(t)=\frac{We}{12}+e^{-t/t_d}\left\{\left(y(0)-\frac{We}{12}\right)\cos\bar{\omega}t+\left(\frac{\dot{y}(0)}{\bar{\omega}}+\frac{y(0)-\frac{We}{12}}{\bar{\omega}t_d}\right)\sin\bar{\omega}t\right\} \tag{2}$$

where

$$t_d=\frac{2\rho_L r^2}{5\mu_L}$$

$$\bar{\omega}=\sqrt{\frac{8\sigma}{\rho_L r^3}-\frac{1}{t_d^2}}$$

O'Rourke and Amsden (1987) argued that when the value of y reaches unity, the droplet breaks up into smaller droplets with a distribution of sizes specified from an energy balance.

The breakup times that the TAB model predicts are of interest. For an inviscid liquid Eq. (2) shows that $y>1$ implies that

$$We=We_{crit}>12 \tag{3}$$

which agrees with the experimental criterion for the onset of bag breakup of Wu el al. (1993). When We is close to this critical value the breakup time is determined from Eq. (2) by assuming that $t_{bu}=\pi$ (where t_{bu} is the breakp time), or

$$t_{bu}=\frac{\pi}{2}\sqrt{\frac{\rho_L r^3}{2\sigma}} \tag{4a}$$

For $We\gg 1$, the drop is assumed to break up after a short fraction of its oscillation period (i. e., $t_{bu}\ll 1$) and, when $y=1$ is assumed, Eq. (2) reduces to

$$t_{bu}=\sqrt{3}\frac{r}{U}\sqrt{\frac{\rho_L}{\rho_g}} \tag{4b}$$

assuming an inviscid liquid. Equation (4b) agrees with the form of "stripping" breakup time correlations proposed by Ranger and Nicolls (1969) and others.

3.2 Wave breakup model

Drop breakup mechanisms are fairly well understood for low speed drops. However there is more uncertainty about breakup mechanisms for high speed drops. The high resolution photographs of Liu and Reitz (1993) indicate that wave

growth processes are involved in the breakup of high speed drops in the 'catastrophic' breakup regime. Liu and Reitz (1993) argued that these waves could originate either from Rayleigh-Taylor (RT) or Kelvin-Helmholtz (KH) instabilities, but they were unable to distinguish between the two instability modes because of uncertainties about the drop's instantaneous velocity and acceleration. The use of double-pulse photography in the present study provides additional data about the drop's dynamics to shed new light on the breakup mechanisms, as described in the next section.

Rayleigh-Taylor instabilities are found when a liquid-gas interface (i. e., a density discontinuity) is accelerated toward the low density gas (Taylor, 1950). The problem is analyzed by considering the unstable growth of infinitesimal surface disturbances on an interface of incompressible fluids. Solutions to the linearized hydrodynamic equations yield a dispersion equation which can be solved to give the wavelength, λ, and growth rate, ω, of the most unstable surface waves, as

$$\lambda = 2\pi\sqrt{\frac{3\sigma}{a(\rho_L-\rho_g)}} \tag{5}$$

$$\omega = \sqrt{\frac{2[a(\rho_L-\rho_g)]^{3/2}}{3\sqrt{3}\sigma(\rho_L+\rho_g)}} \tag{6}$$

where, a, is the drop's acceleration.

On the other hand K-H instabilities are generated when a high relative velocity exists at the interface between the liquid and gas flows. Liu and Reitz (1993) have suggested that wave crest stripping of KH instability waves may account for the extremely small drops that are found in high speed drop breakup. Reitz (1988) generated curve fits of the numerical solution for the maximum growth rate, Ω, and for the corresponding wavelength, Λ, where

$$\frac{\Lambda}{r} = 9.02\frac{(1+0.45Z^{0.5})(1+0.4T^{0.7})}{(1+0.87We_2^{1.67})^{0.6}} \tag{7}$$

$$\Omega\left[\frac{\rho_1 r^3}{\sigma}\right]^{0.5} = \frac{0.34+0.38We_2^{1.5}}{(1+Z)(1+1.4T^{0.6})} \tag{8}$$

and $Z = We_1^{0.5}$, $T = ZWe_2^{0.5}$, $We_1 = \rho_1 U^2 r/\sigma$, $We_2 = \rho_2 U^2 r/\sigma$ and $Re_1 = Ur/\nu_1$.

Liquid breakup has been modeled by postulating that new drops are formed from the bulk liquid or "blob" with drop diameters proportional to the wavelength of the fastest growing or most probable unstable surface wave. In this case, the characteristic time of breakup of surface waves is

$$\tau = \frac{3.726B_1 r}{\Lambda\Omega} \tag{9}$$

where B_1 is a breakup time constant. It can be shown that Eq. (9) reduces to Eqs. (4a) and (4b) in the low and high Weber number limits with $B_1 = 1.35$ and $B_1 = \sqrt{3}$, respectively, for an inviscid liquid.

4. Results and Discussion

High-magnification pulsed-illumination photographs were taken of the drop breakup process to reveal drop breakup mechanisms under high speed air stream condition. In addition, drop accelerations and drop trajectories were measured from the photographic results discussed below.

4.1 Breakup mechanisms

Double-pulsed illumination high-magnification photography was used to examine the temporal breakup process. The time interval between the two flash pulses was varied from 1 to 20 μs since the time interval between monodisperse droplets arriving at the air jet was about 20 μs. As mentioned earlier, the two light flashes had different intensities which was used to differentiate each event. The first picture is brighter (lighter) than the delayed second picture.

Figure 3 depicts the temporal breakup process under room temperature conditions when the air jet velocity was 70, 150 and 200 m/s, Cases 1, 2 and 3 in Table 1, respectively, using four different time delays of 20, 10, 5 and 1 μs between flashes. The lighter images are from the first spark and delayed second images are darker. The drops enter the air jet at the upper right-hand-corner of each frame. Figure 3(a) shows the characteristics of drop breakup in the bag breakup regime. The injected drops begin being flattened by the nonuniform pressure distribution on their surface soon after they enter the air jet. The formation of the bag starts about 65 μs after the drops enter the

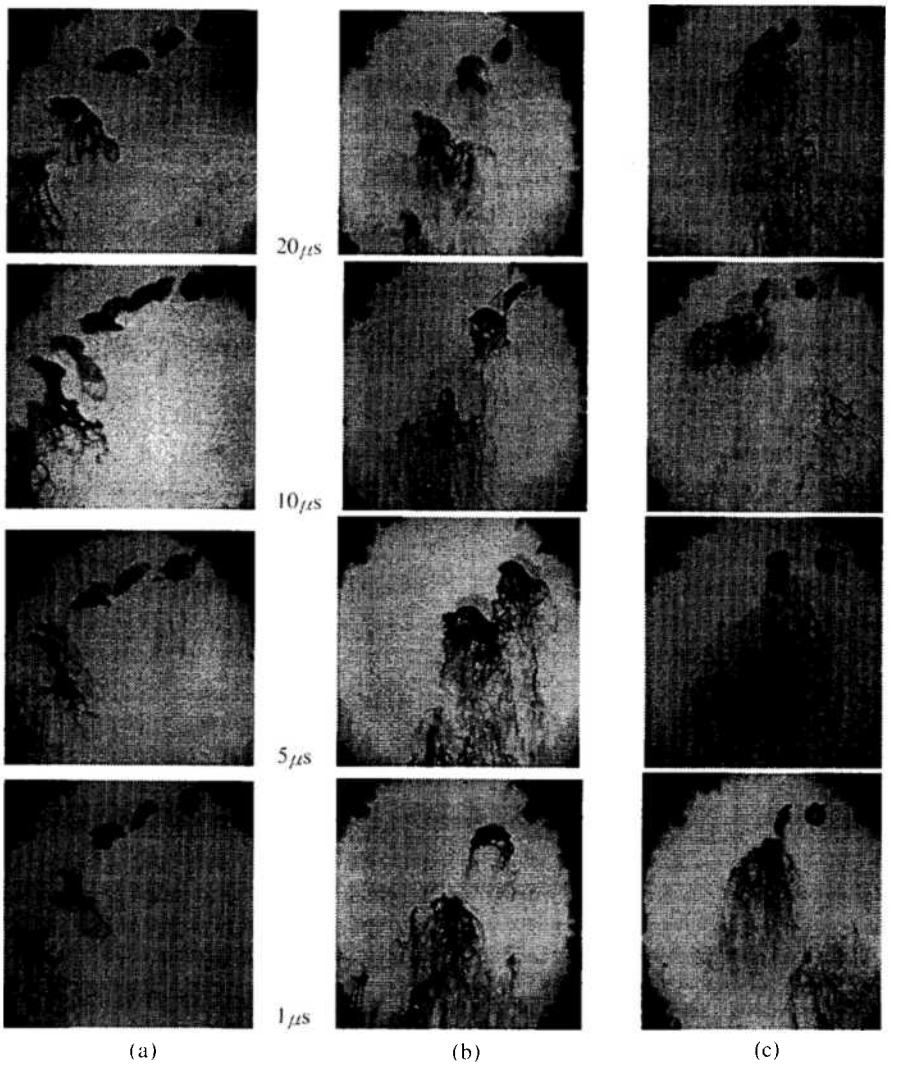

Fig. 3 Double pulse photographs at 70 m/s(a), 150 m/s(b), 200 m/s(c) with different time intervals between pulses

air jet. The bag consists of liquid that presumably originates from the thinnest point of the flattened drop. The time of bag formation is shorter than the breakup time estimated from Eq. (4a) which predicts that the drop is broken up (i. e., y reaches unity) when $t_{bu}=208$ μs. Equation (4a) considers only the natural frequency of oscillation of the drop and does not consider the air velocity. Equation (4b) accounts for the dynamic pressure effect due to the air jet velocity and predicts a breakup (or flattening) time of 60.5 μs, which agrees much better with the observed bag formation time.

Once the bag is formed it is swept downstream. A network of filaments can be seen in Fig. 3(a) to be superimposed on the surface of the extended bag and the filaments eventually become isolated ligaments when the bag is ruptured.

Figure 3(b) (air velocity of 150 m/s) shows breakup in the boundary stripping or shear breakup regime. Again considerable flattening of the drop is seen to have occurred in times of the order of 20 to 25 μs. The predicted flattening time of the drop from Eq. (4b) is 28.2 μs, which again agrees

quite well with the data.

As can be seen, in this case a liquid sheet appears to be stripped away from periphery of drop (see the initial stages of breakup in the 20 and 10 μs frames). Filaments are also seen to exist on the surface of this sheet. The filaments eventually become discrete ligaments as the sheet is stretched in the downstream direction by the air flow.

Breakup in the 'catastrophic' breakup regime is shown in Fig. 3(c). In this case, the flattening process occurs even more very rapidly. The drop changes to the shape of a liquid sheet in 15 to 20 μs after the high velocity flow hits the droplet. Considerable breakup of the drop is seen to have occurred within 25 μs after the drop enters the air jet (recall that the temporal spacing between drops entering the air jet is 25 μs). The prediction of Eq. (4b) for the flattening time of the high speed drop is $t_{bu}=21.2$ μs, which is again consistent with the measurement data.

Magnified images of Cases 1, 2 and 3 taken with 10, 20 and 10 μs between flashes, respectively, are reproduced in Fig. 4 to allow the breakup process to be seen more clearly. Figure 4(a) shows the bag breakup details after about 65 and 75 μs from the time the drop entered the air jet. The images clearly shows the transition from a bag to the appearance to ligaments. The inflated bag-shaped liquid sheet bursts into ligaments whose direction are almost aligned with the air-flow direction. This is different from the breakup that results from the growth of capillary instabilities on liquid sheets because, in that case, the ligaments are perpendicular to liquid flow direction. The present results indicate that other mechanisms need to be included in instability theories of liquid sheets to explain the results.

Breakup in the boundary stripping or shear regime is shown in Fig. 4(b). In this case the liquid film at the periphery of the drop is also seen to breakup into ligaments, which are roughly aligned with the flow direction. In this breakup regime, the normal and shear stresses at liquid surface and the surface tension need to be considered in order to describe the physics of the formation of the liquid sheet.

Figure 4(c) shows breakup in the 'catastrophic' breakup regime. The very interesting phenomena which were also found by Liu et al.(1993) are seen on the drop surface. As can be seen, large-scale instability waves are visible on the windward surface of droplet.

The details of the later stages of the breakup process are shown in Fig. 5 which shows single-pulse illumination photographs taken using the second field of view indicated in Fig. 1. The field of view is such that the lower speed drops actually exit through the other side of the air jet. As can be seen, in the bag breakup regime, the ligaments are continuously elongated, and the breakup length is very large. In the stripping and 'catastrophic' regimes, the breakup length of the ligaments are much shorter due to high air velocity.

At very high air velocities, the drop experiences a large dynamic pressure change on its surface. A similar situation is found when a stationary drop is exposed to a shock wave or a high-intensity sound wave. Anilkumar et al.(1993) found large scale instability waves were generated on the flattened droplet surface under acoustical levitaion. However, these waves were thought to result from a resonance between azimuthal and radial capillary waves on the drop's surface. In the present experiments the drop is undergoing an intense acceleration instead of an acoustic excitation. These conditions favor the development of Rayleigh-Taylor instabilities. Since double pulse-illumination was used in the present experiments it is possible to estimate the acceleration of the drops and, using Eqs. (5) and (6), to estimate the wavelengths and growth rates predicted by the RT wave theory for comparison. This is shown, for example, in Fig. 6 and in Table 2. For the conditions of Case 3 in Fig. 6 the measured wavelength is 58.7 μm. This agrees reasonably well with the prediction of Eq. (5) listed in Table 2 of 39.3 μm. The acceleration of the drop was determined from the double-pulsed images to be about 1.9×10^5 m/s^2 (see Table 2) with an uncertainty in the determination of the acceleration estimated to be about 20%. In addition, the predicted wave growth rate of 2.2 μs shown in Table 2 is also consistent with estimates of wave

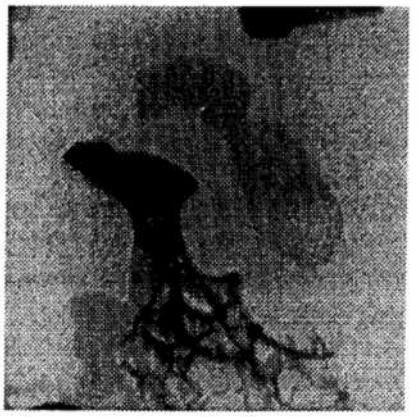

Case 1 (a)

Case 1 (a)

10 μs

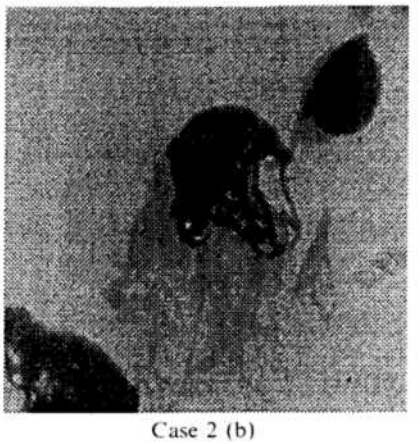

Case 2 (b)

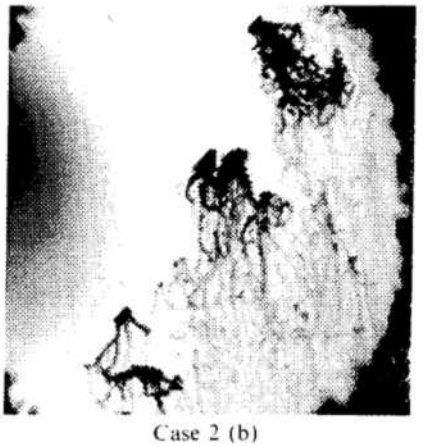

Case 2 (b)

20 μs

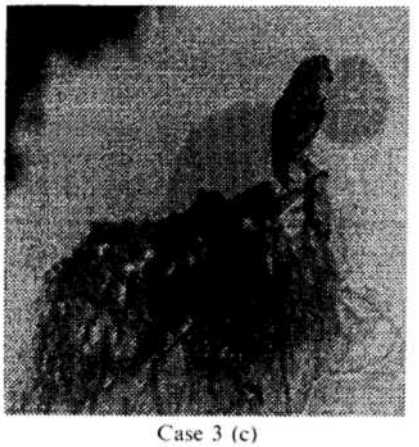

Case 3 (c)

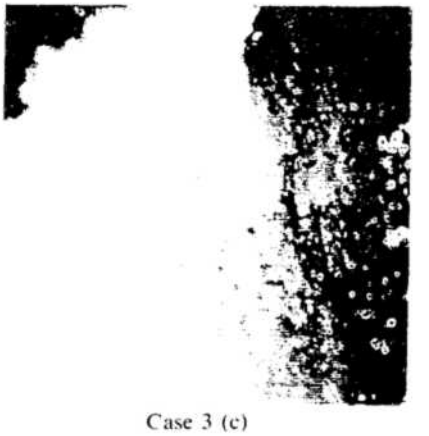

Case 3 (c)

10 μs

Fig. 4 Magnified views of breakup at three break at (a) 70 m/s (b) 150 m/s and (c) 200 m/s

Fig. 5 Single pulse photographs of breakup in three different breakup regimes (a) 70 m/s, (b) 150 m/s and (c) 200 m/s using second field of view

growth rates obtained from the photographs. As seen in Fig. 3(c), with the 10 μs interval between images, the drop surface shows no appearance of any instability waves in the illumination from the first pulse. The waves are clearly visible in the illumination from the second pulse 10 μs later in time.

The comparison between predicted and measured wavelengths from the present photographs indicates that it is likely that the large wavelength waves seen in the 'catastrophic' regime are RT waves. Theoretically, RT waves originate on the leeward surface of an accelerating drop. However, in the present case the drop is flattened into the form of a sheet, and it is reasonable to expect that the RT waves would also appear on the windward surface if the sheet thickness was small in comparison to the wavelength, as is probably the case in the present study. Unfortunately, there does not appear to be a complete theory available at the present time for predicting the stability of an accelerating, thinning, liquid sheet.

As can be seen in Table 2 the wavelengths (and growth rates) of KH waves are predicted to be much shorter (i. e., 5.92 μm) than the wavelength derived from the photographs. For Table 2, the KH wave estimates were made using Eqs. (7) and (8) using the initial drop-gas relative velocity (i. e., the air-jet velocity). This is reasonable since the velocity of the drops is much less than the velocity of the air-jet at early times (e. g., the instantaneous velocity of the drop studied in Fig. 6 is estimated to be about 40 m/s which is still much lower than the gas velocity which is 200 m/s). Moreover, the air velocity at the drop's equator would be expected to be even higher than the jet velocity because of the nature of a stagnation point flow around the drop. Thus, the estimates of KH wavelengths and growth rates in Table 2 are likely to overstimates.

Fig. 6 Details of surface wave development in 'catastrophic' breakup regime. The measured wavelength is $\lambda = 58.7$ μm

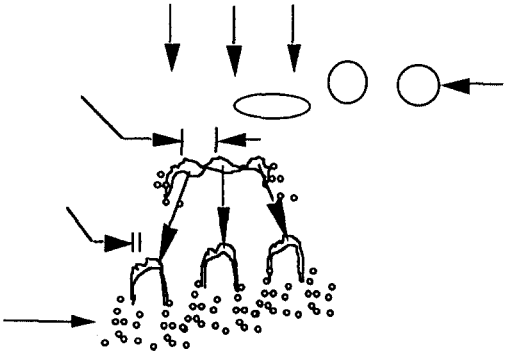

Fig. 7 Schematic diagram of breakup mechanisms in 'catastrophic' breakup regime

Table 2 Predicted Kelvin-Helmholtz and Rayleigh-Taylor wave lengths and growth rates

	Kelvin-Helmholtz		Rayleigh-Taylor		
Case/velocity(m/s)	$\Lambda(\mu m)$	$1/\Omega(\mu s)$	$\lambda(\mu m)$	$1/\omega(\mu s)$	Acceleration $\times 10^{-4}$(m/s^2)
1- 70	42.5	5.80	82	7.33	38.4
2-150	10.0	0.71	54.6	3.94	88.0
3-200	5.9	0.35	39.3	2.23	189.6

The above analysis using double-pulsed photography reveals that the breakup mechanism in the 'catastrophic' breakup regime consists of a series of characteristic processes in which the aerodynamic force on the drop flattens the drop into the shape of a liquid sheet. The accelerating sheet breaks into large-scale fragments by means of RT instability. Apparently much shorter wavelength KH waves originate at the edges of the fragments and these waves are stretched to produce ligaments which then breakup into the micron size drops that have been measured in this regime (Liu and Reitz, 1993). These processes are illustrated schematically in Fig. 7.

5. Summary and Conclusions

A well controlled experiment has been performed using double-pulsed short-duration photography to study the breakup mechanisms of high speed drops. The experiments provided information about breakup mechanisms for comparison with mechanistic models.

The following conclusions have been obtained.

① The mechanism of drop breakup consists of a series of processes that start when the drop is initially flattened by the aerodynamic force caused by its relative motion with the gas. The time of flattening of the drop is well predicted by the Taylor Analogy TAB model in all three drop breakup regimes.

② Once the drop is flattened in the bag breakup regime a bag is produced, which presumably originates from the thinnest point of the flattened drop. The bag is blown-out in the downstream direction and, when it ruptures, ligaments are produced which are aligned with the air-flow direction. In the shear breakup rigime, a sheet or curtain is formed at the equator of the flattened drop. Once again, ligaments are formed from the fragmentation of the sheet, and the ligaments are aligned with the air-flow direction. The lignment of the ligaments is different from that postulated in classical studies of the breakup of liquid sheets where the ligaments are aligned perpendicular to the flow direction.

③ There is more uncertainty about drop breakup mechanisms in the 'catastrophic' regime. A previous study (Liu and Reitz, 1993) showed that long wavelength waves were involved in the breakup process. It was proposed that the breakup could be due to the unstable growth of Rayleigh-Taylor (RT) or Kelvin-Helmholtz (KH) waves. The double-pulse illumination photography used in the present study has helped clarify the breakup mechanism further. Relatively long wavelength RT waves appear to fragment the accelerating flattened drop. Short wavelength KH waves grow on the surfaces of the fragments and produce ligaments which are stretched in the flow direction. The ligaments breakup to produce the minute (micron-sized) drops that are found in the 'catastrophic' breakup regime.

Acknowledgment

The author greatly acknowledges to the financial support of Research Fund of University of Inchon for this work. The author thanks Prof. Reitz of University of Wisconsin for help with the paper.

References

Anilkumar, A. V., Lee, C. P. and Wang, T. G., 1993, "Stability of an Acoustically Levitated and Flattened Drop : An Experimental Study," *Physics of Fluids*, A5(11), pp. 2763~2774.

Berglund, R. N. and Liu, Y. H., 1973, "Generation of Monodisperse Aerosol Standards," *Experimental Science & Technology*, Vol. 7, No. 2, pp. 147~153.

Hsiang, L. P. and Faeth, G. M., 1992, "Near Limit Drop Deformation and Secondary Breakup," *Atomization and Spray*, Vol. 8, No. 5, pp. 635~652.

Kennedy, J. B. and Roberts, J., 1990, "Rain Ingestion in a Gas Turbine Engine," *Proceedings of 4th ILASS Meeting*, May 21~23, Hartford, CT., p. 154.

Krzeczkowski, S. A., 1980, "Measurement of Liquid Droplet Disintegration Mechanism," *Int. J. Multiphase Flow*, Vol. 6, pp. 227~239.

Liu, A. B. and Reitz, R. D., 1993, "Mechanism

of Air Assisted Liquid Atomization," *Atomization and Spray*, Vol. 3, pp. 55~75.

Mahoney, T. J. and Sterling, M. A., 1978, "The Breakup Length of Laminar Newtonian Liquid Jets in Air," *ICLASS-1978*, Tokyo.

O'Rourke, P. J. and Amsden, A. A., 1987, "The TAB Method for Numerical Calculation of Spray Droplet Breakup," *SAE Paper* 872089.

Pilch, M. and Erdman, C. A., 1987, "Use of Breakup Time Data and Velocity History Data to Predict the Maximum Size of Stable Fragments for Acceleration-Induced Breakup of Liquid Drop," *Int. J. Multiphase Flow*, Vol. 13, pp. 741~757.

Ranger, A. A. and Nicholls, J. A., 1969, "The Aerodynamic Shattering of Liquid Drops," *AIAA J.*, Feb.,Vol. 7, pp. 285~29.

Rayleigh, W. S., 1878, "On the Instability of Jets," *Proc. Lond. Math. Soc.*, Vol. 4, p. 10.

Reitz, R. D., 1988, "Modeling Atomization Processes in High-Pressure Vaporizing Sprays," *Atomization and Spray Technology*, Vol. 3, pp. 309~337.

Reitz, R. D. and Bracco, F. V., 1986, "Mechanism of Breakup of Round Liquid Jets," in *Encyclopedia of Fluid Mechanics*, Gulf Pub, Houston, TX. p. 233.

Taylor, G. I., 1950, "The Instability of Surfaces When Accelerated in a Direction Perpendicular to Their Planes. I.," *Proc. Roy. Soc.* A, Vol. 201, pp. 192~196.

Wu, P. K. and Faeth, G. M., 1993, "Aerodynamic Effects Primary Breakup of Turbulent Liquids," *Atomization and Sprays*, Vol. 3, pp. 265~289.

Wu, P.-K., Hsiang, L.-P. and Faeth, G. M., 1993, "Aerodynamic Effects on Primary and Secondary Spray Breakup," *First International Symposium on Liquid Rocket Combustion Instability*, Pennsylvania State University, University Park, PA.